

# Estimate of ground support response under dynamic loads at El Teniente mine, Codelco, Chile

MS Celis *Codelco, Chile*

RA Parraguez *Codelco, Chile*

## Abstract

*The dynamic loads associated with the occurrence of seismic events in primary rock mass resulting from caving exist throughout the service life of the drifts, sometimes damaging the ground support system. To estimate the ground support response under dynamics loads, a Factor of Safety (FS) is estimated analytically that seeks to characterise these dynamic loads in terms of ejection velocities and thickness of damage, while quantifying the energy dissipation capacity of the ground support systems, finally making with these values an energy balance.*

*Through field back-analysis, it is sought to characterise these dynamic loads in terms of ejection velocities and damage depth. To complete the analysis, over time it has been sought to quantify the energy dissipation capacity of the ground support systems and thus be able to represent numerically, estimating a FS with an energy balance, the response of the installed support. It has not been easy to perform these analyses because the process of load transfer to the support and its response is a complex process that includes several assumptions and multiple variables, such as the rock mass failure mode, failure mode of reinforcement elements, anchoring and retention system. Today, to represent the response of the ground support systems, reproduction of the laboratory boundary and load conditions have been sought. The quality of the installation of the support system is also reviewed as a variable. This is a factor that in some cases has conditioned the response to this type of load. What is sought with this analysis is to empirically represent what was observed in the field, aiming to introduce improvements in ground support systems or requirements for new support elements. Some examples are presented where the response of the ground support has been estimated with field data, the limitations when doing the analysis, the improvements introduced in the current ground support systems (among others, reinforcement and retaining elements with greater energy dissipation capacity) and finally, the challenges to improve these evaluations are presented.*

**Keywords:** *ground support, dynamic load, support installation quality*

## 1 Introduction

The response of ground support systems to dynamic stresses or seismic events associated with mining in the environment has not always been the same. It clearly depends on the seismic parameters that characterise the dynamic load (mainly magnitude, energy, and location) and on the ground conditions (section size, pillar geometry, geological characteristics).

In this context, through back-analysis, it is sought to characterise the dynamic load represented on the ground by the ejection velocity that can be obtained from the mass projection evidences and by the damage thicknesses that remain visible after material projection. On the other hand, to complete an energy balance, the energy dissipation capacity of the support elements and systems is also considered.

Empirically representing the response of the ground support is sought. Assumptions are made in this process since it is very difficult to quantify all the variables. This Factor of Safety (FS) should reflect the response that has been observed in the field.

Over time, the difficulties in carrying out this analysis have become evident, but we can increase the FS by introducing improvements in ground support designs, promoting the search for new elements or support systems and giving more significance to the quality controls of the ground support installation.

For a couple of real cases, the analysis carried out from which the following challenges are posed to improve these evaluations will be shown.

## 2 Estimation of the ground support response and assumptions for the analysis

To represent the response of the support to dynamic loads, a FS is calculated as the ratio between the available energy (energy dissipation capacity of the ground support system) and the loading energy (dynamic load).

$$FS = \frac{\text{Available Energy}}{\text{Loading Energy}} \tag{1}$$

Next is the description of how both energies (available and loading) are estimated to obtain the FS.

### 2.1 Energy available: energy dissipation capacity of the ground support system

The current ground support systems at the El Teniente mine systematically include the use of steel bolts, galvanised mesh, and shotcrete, as shown schematically in Figure 1.

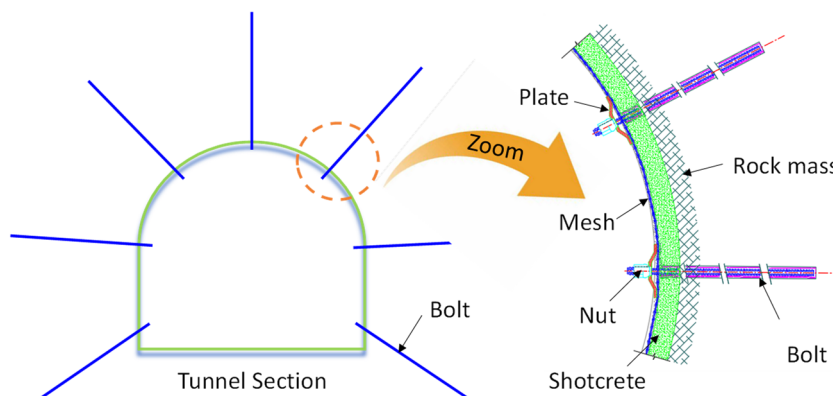


**Figure 1 Bolt-mesh-shotcrete design**

In the areas with greater section that occurs at the drift intersections, the preceding support with bolts, mesh and shotcrete is complemented with steel cable bolts installed in the roof, as shown in Figure 2.

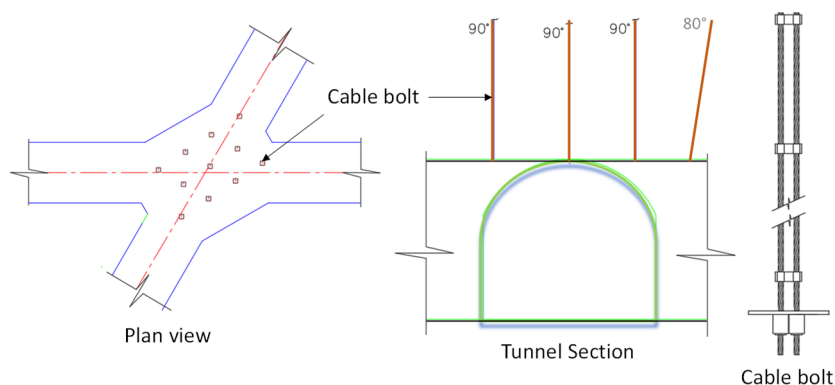


**Figure 2 Cable bolt design**

The technical specifications of bolts, mesh, shotcrete and cable bolts are summarised in Table 1.

**Table 1** Technical specifications of support elements

Element	Support specifications
Bolt	Steel quality: A440-280H (A: steel, H: concrete). Diameter: 22 mm. Tensile strength: 4,400 kg/cm <sup>2</sup> . Ultimate force: 16 t. Fluency force: 12 t. Length: variable between 2.3–3.5 m. Pattern: 1 × 1 m.
Cable bolt	Steel quality: ASTM A 416. 270K grade. Diameter: 15.2 mm. Tensile minimal load: 23 t. Length: variable between 8–12 m. Pattern: 2 × 2 m. Two cable bolts in one borehole.
Mesh	Chain link mesh. Gauge wire BWG 6. Minimum wire resistance: 373 N/mm <sup>2</sup> .
Shotcrete	Compressive strength: 225 kg/cm <sup>2</sup> (age 28 days). Thickness 5 cm under mesh plus coating thickness 1 cm.

The energy dissipation capacity is defined as the area under the load elongation curve of an element subjected to axial load. Considering laboratory results, the following energy dissipation capacities are assumed for the support elements in Table 1.

The values in Table 2 (Rojas et al. 2015) are obtained from a dynamic test setup where a tensile load is applied and which seeks to reproduce the boundary and load conditions present in the field. This is very difficult, since it intends to reproduce a dynamic load or variable condition in time that acts on the support and that also has complex boundary conditions, such as a heterogeneous rock mass that can range from a disassembly of blocks to a bigger size wedge. It is also complex because what is sought to be tested is a ground support system and not isolated support elements.

**Table 2** Energy dissipation or support capacity

Element	Value
Bolt	22 kJ (diameter 22 mm, steel quality: A440-280H)
Cable bolt	12–16 kJ (steel quality: 270K grade, diameter: 15.2 mm)
Mesh	8–12 kJ (chain link mesh. Gauge wire BWG 6)

Over time, improvements have been made to this laboratory test, seeking to bring it closer to the real field condition.

Regarding the failure modes for bolts and cable bolts, failures due to shear stress, tensile stress or a combination of both have been observed in the field, as presented in Figure 3.

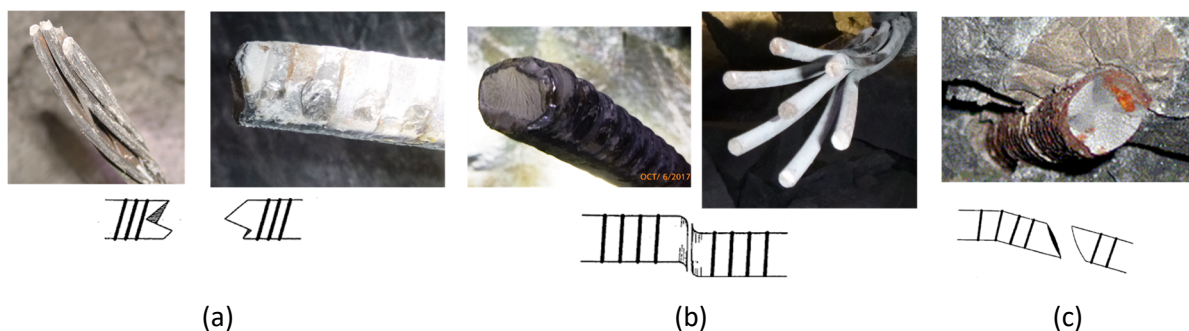


**Figure 3** Bolt and cable bolts failure modes. (a) Tension; (b) Shear; (c) Tension and shear

The dissipation capacity of the ground support system is estimated as the sum of the individual contributions of each element:

$$\text{Energy} \left[ \frac{kJ}{m^2} \right] = \sum \frac{E_{bolts}}{\text{area}} + \sum \frac{E_{cable\ bolts}}{\text{area}} + \sum \frac{E_{mesh}}{\text{area}} \quad (2)$$

In Equation 2, area refers to the surface where the dynamic load is assessed or damage to the support system is observed.

If a failure is observed on the ground due to a combination of shear–tensile stress, the value of tension load in Table 2 is weighted by 0.65. This value considers what is established in the AISC-ASD89 code, which indicates that the shear strength ( $F_{shear}$ ) is estimated as 40% of the yield strength, which, for bolts with a diameter of 22 mm ( $F_{tension} = 16\text{ t}$ ) with a steel quality of A440-280H, is calculated as:

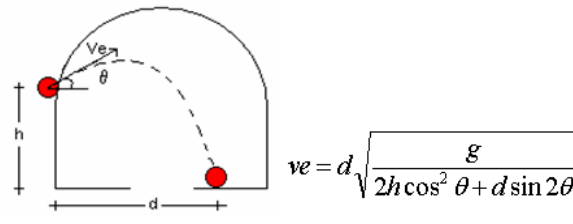
$$F_{shear} = 0.4 \times 16 = 6.4\text{ t} \quad (3)$$

$$\frac{F_{shear} + F_{tension}}{2} = \frac{6.4 + 16}{2} = 11.2\text{ t} \approx 0.65 \times F_{tension} \quad (4)$$

## 2.2 Loading energy: dynamic load

To estimate the loading energy, the ejection velocity ( $ve$ ) and the damage thickness ( $e$ ) are needed as input data.

The ejection velocity ( $ve$ ) can be estimated by recording on the ground the distance ( $d$ ) and height ( $h$ ) at which a shotcrete slab was projected from the supported sector. With these data, applying the projectile motion formula, the ejection velocity ( $ve$ ) can be calculated.



$$ve = d \sqrt{\frac{g}{2h \cos^2 \theta + d \sin 2\theta}} \quad (5)$$

where:

$\theta$  = angle of the particle with respect to the horizontal plane.

$G$  = gravity =  $9.8\text{ m/s}^2$ .

The main variables in Equation 5 are distance ( $d$ ) and height ( $h$ ). The value of the projection angle of the particle with respect to the horizontal plane ( $\theta$ ) does not affect the ejection velocity ( $ve$ ) for a range of 30–40°.

It is very difficult to estimate  $ve$  in the field because it is not possible to define the point from which a block or particle is projected. However, at Pilar Norte, Esmeralda and Reno mines at El Teniente (Table 3), the projection of concrete blocks (Figure 4) with known geometry was recorded, for which it was easy to calculate ( $ve$ ) values with projectile motion Equation 5. These are currently used as references for this analysis (Rojas et al. 2020; Van Sint Jan 2005).

**Table 3** Historical values of ( $v_e$ ) in El Teniente mine

Date	Value	Sector	Damage classification
November 2009	4 m/s	Pilar Norte	Minor
December 2009	9 m/s	Pilar Norte	Severe
January 2010	7 m/s	Pilar Norte	Severe
February 2017	2–3 m/s	Pilar Norte	Minor
November 2009	4 m/s	Esmerelda	Minor
August 2005	6 m/s	Reno	Severe

**Figure 4** Concrete mass ejection in Pilar Norte El Teniente. (a) January 2010; (b) February 2017

In the case of the damage thickness ( $e$ ), it is easier to obtain its value in the field (an example of which is presented in Figure 5), since the overbreak resulting from the projection of rock mass blocks can be measured, and then, with that value and taking into account the rock density  $2.7 \text{ t/m}^3$ , the mass ( $m$ ) per area unit will be quantified.

**Figure 5** Ground thickness of damage

Finally, the dynamic load characterised as the loading energy, corresponds to the kinetic energy calculated as:

$$\text{Dynamic Load} = \text{kinetic energy} \left[ \frac{\text{kJ}}{\text{m}^2} \right] = \frac{1}{2} \times m \times v_e^2 \quad (6)$$

### 2.3 Factor of Safety

With Equations 2 and 6, it is possible to estimate the value of the FS.

What is sought with the estimation of this factor is to reproduce what was observed in the field, so that the analysis carried out makes sense. Put another way, it is expected to estimate values less than 1.0 for the sectors where there has been a failure of the ground support elements.

### 2.4 Information of seismic sensors network

At El Teniente mine there is currently a network of seismic sensors (geophones–accelerometers), which online provide information on the occurrence of seismic events in the different sectors of the mine. In this manner, the seismic event parameters such as location, magnitude, and energy, among others, are identified. This seismic network is systematically maintained, which includes the installation of new sensors according to the needs associated with the progress of mining.

The seismic information is necessary for the evaluation of blasting, delimitation of safety zones for workers' protection and for the geomechanical control of the caving progress.

When a rockburst is recorded, the first thing that is done is to identify the focus of the seismic event (mine coordinates) and with this, a first correlation is made with the sectors with damage.

Historically, what has been seen is that the distribution of damage on the ground does not follow a defined pattern. This can be associated with the fact that the seismic wave propagation is not circular but rather elliptical (Figure 6), which means that points located at the same distance from the source of the event have different responses (with or without damage to the support system). Other factors also affect this last point, such as the orientation or size of the drifts and their local condition in terms of geological characterisation or state of the installed ground support.

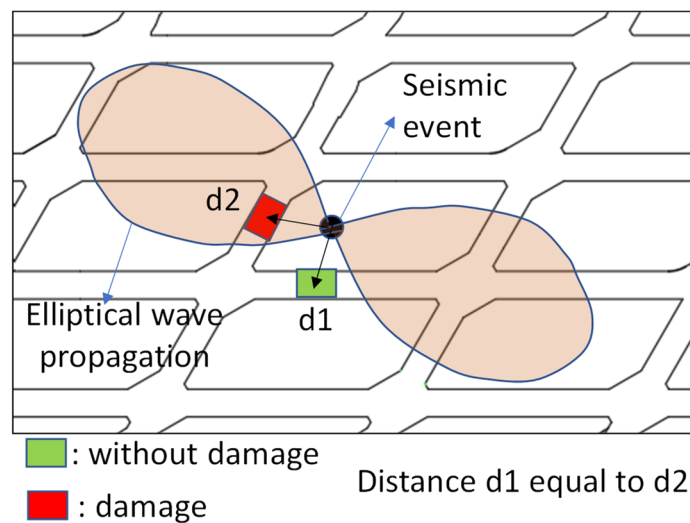


**Figure 6 Elliptical wave seismic event propagation**

The geophones particle velocity ( $ppv$ ) readings are shown as an example in Figure 7.

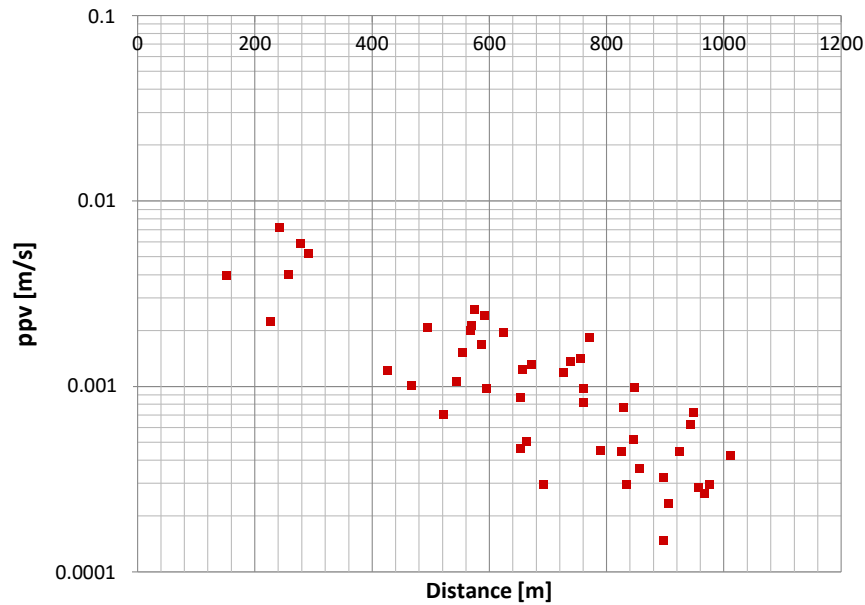


**Figure 7 Graphic distance versus magnitude**

The damages occur in the ‘near field’, that is, at a distance less than 50 m from the focus of the event for which there is no reading from the geophones as they are installed far from the mining to avoid being damaged.

If we had the ‘near field’ information, we would still have to add more assumptions to obtain from the particle velocities ( $ppv$ ) the ejection velocity ( $ve$ ) that is required for this analysis, since the geophones are installed at depth (8 m inside the borehole) so there is an amplification factor for the  $ppv$  of which today, in the literature, there is no consensus regarding its value (it could vary between 3 and 50) and thus obtain  $ve$ .

To evaluate the ground support response, the values in Table 3 are considered with the relationship between the magnitude and the energy of events for which damage has been recorded in the support described in Table 1 at El Teniente mine, as shown in Figure 8.

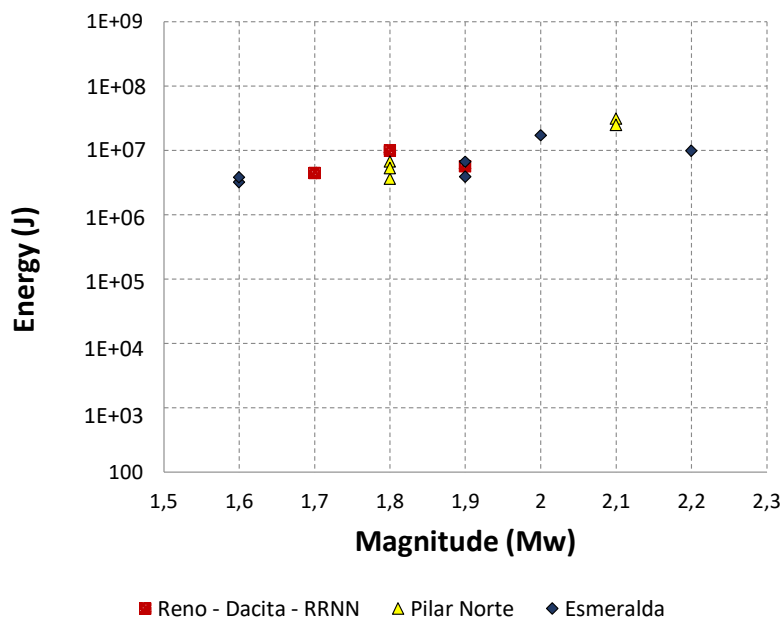


**Figure 8 Support failure statistic**

Figure 8 considers only rock bursts as of October 2015 due to a change in the event processing system.

### 3 Real cases

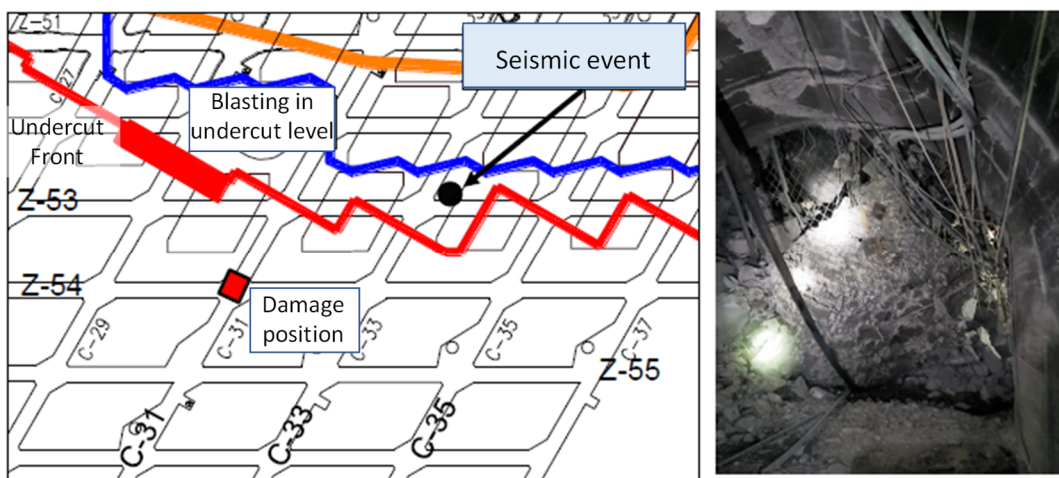
The ground support response is estimated after two rock bursts:

1. Esmeralda mine (October 2020).
2. Pacífico Superior mine (February 2023).

#### 3.1 Esmeralda mine rockburst: 5 October 2020

At the end of 5 October 2020, an undercutting blast was fired. Along with the blasting, a seismic event of magnitude  $M_w 1.9$  and energy of  $3.9 \times 10^9$  J was recorded. The focus of the event, located 20 m above the production level, was recorded within the time and safety isolation halo of the area (Celis 2020).

The strong damage associated with this rockburst was located at the production level of Esmeralda mine, at the intersection of two drifts (C-31 with Z-54), as seen in Figure 9.



Damage in intersection C-31/Z-54

**Figure 9** Damage position

The ground support installed in the sector with damage includes elements with the characteristics shown in Table 1: 2.3 m long bolts, 8 m long cable bolts, mesh and shotcrete. The arrangement of bolts and cables bolts corresponds to those shown in Figures 1 and 2.

Figure 10 shows the estimate of the rock mass volume that fell at the intersection.

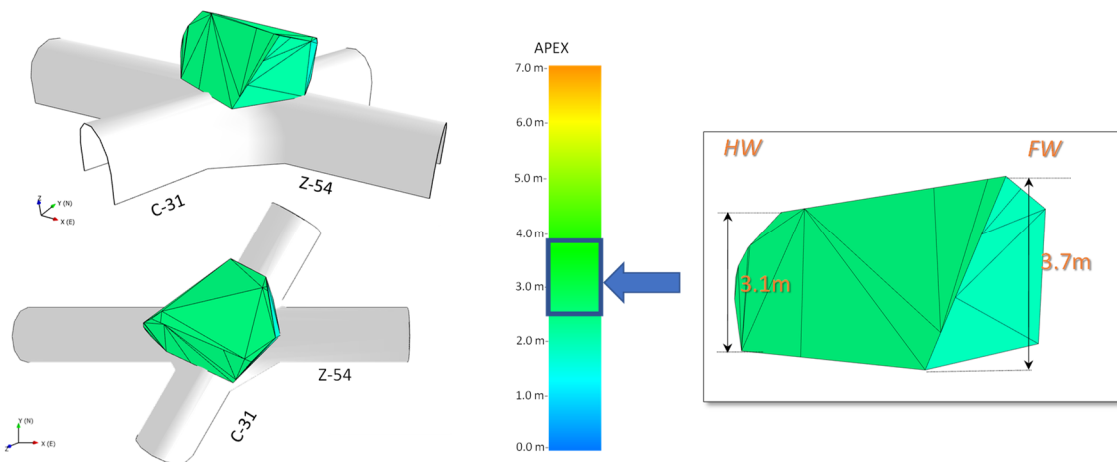


**Figure 10** Estimation of the released volume



The fallen volume limit (apex around 3 m) exceeds the design length of the bolts (2.3 m), so the bolts could not support the weight for this loading and were not considered in the analysis. In the field, complete bolts were observed in the material on the floor (Figure 11). The mass of the fallen volume was estimated at 152 t and the area of the damaged zone was estimated at 30 m<sup>2</sup>.

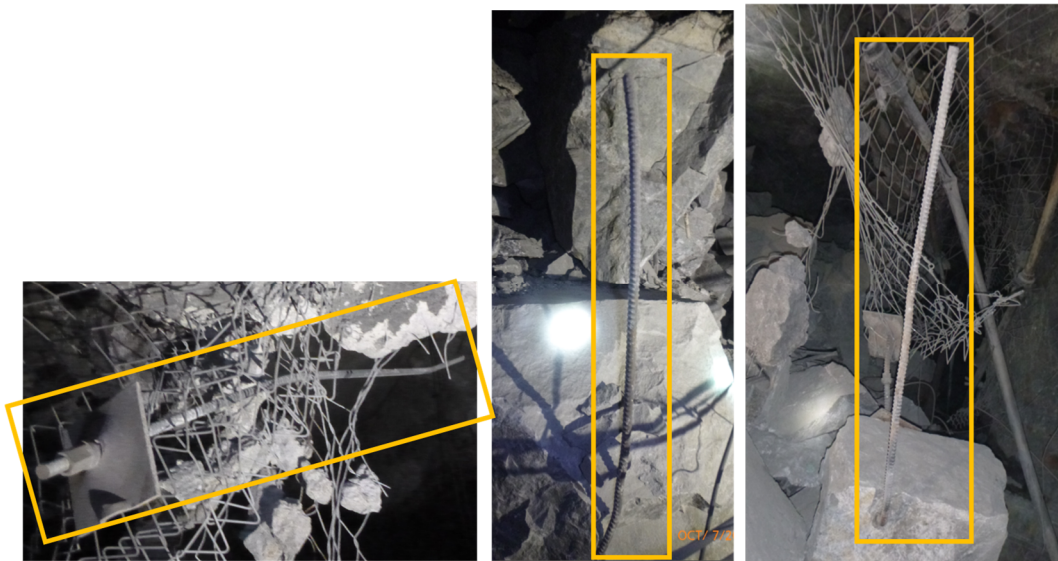


**Figure 11 Complete bolt inside released volume**

With respect to the cable bolts in the roof of the intersection, the following survey was carried out (Figure 12):

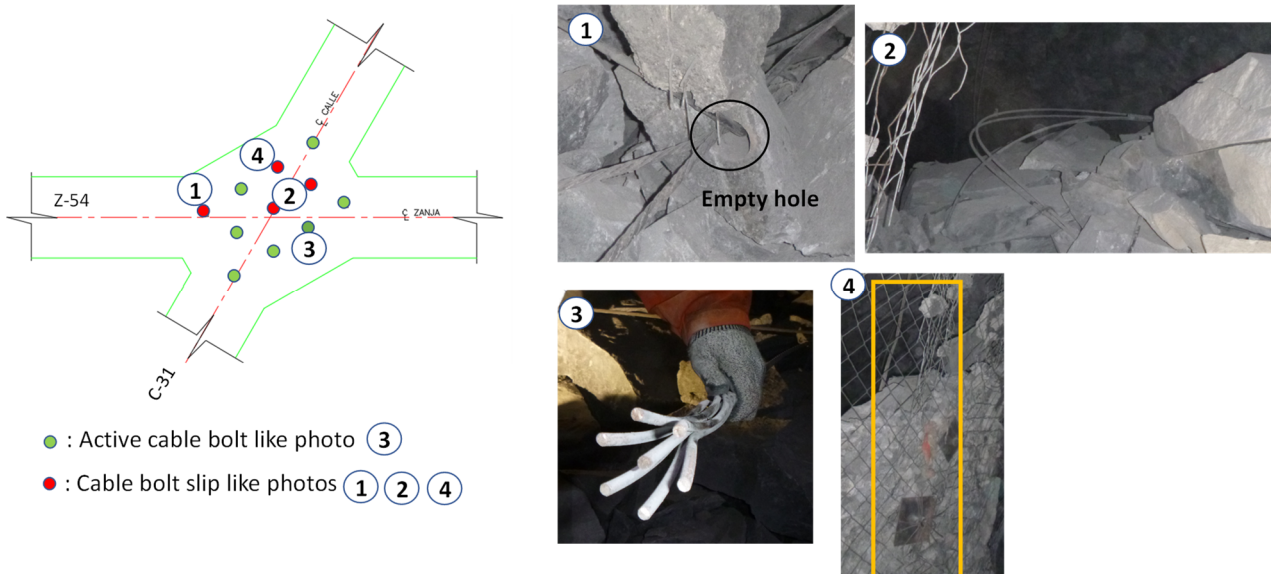


**Figure 12 Cable bolt condition**

In the field, 36% of the design cable bolts slipped due to poor installation quality since these cables were without cement grout or inner anchorage (evidence of empty hole shown in Figure 12).

The ejection velocity could not be estimated with the field data, so considering the level of damage, the lowest of the recorded values (2 m/s) in Table 3 will be considered for (*ve*).

If the FS is estimated for this case, we obtain:

$$Dynamic\ Load = \frac{1}{2} \times \frac{152}{30} \times 2^2 = 10.1\ kJ/m^2 \tag{7}$$

$$\text{Energy} = \frac{16 \times 2 \times 7}{30} = 7.5 \text{ kJ/m}^2 \tag{8}$$

$$\text{FS} \sim 0.7 \tag{9}$$

From the analysis carried out, the following can be concluded:

- The ground support design systematically considers the installation of bolts that are complemented in greater sections with cable bolts, which allow deeper anchoring, where, due to the excavation geometry, the conditions for the formation of larger wedges or landslides occur at greater depth.
- The falling of the volume of rock at the intersection of C-31 with Z-54 at the production level is because 36% of the cable bolts did not achieve their design function since they slipped due to the absence of grout along the cable bolts (poor installation quality).

### 3.2 Pacífico Superior mine rockburst: 1 February 2023

On 1 February 2023, special blasthole blasting was carried out to scale the drawbells with irregular geometry in the sector. After the blasting, a seismic event of magnitude  $M_w 1.4$  and energy of  $2.6 \times 10^5 \text{ J}$  was recorded. The focus of the event, located at the production level, was recorded in an area exclusive to equipment traffic Costanzo et al. (2023).

The strong damage associated with this rockburst (7 m in length) is located at the production level of Pacífico Superior mine in the pillar of an intersection (Figure 13).

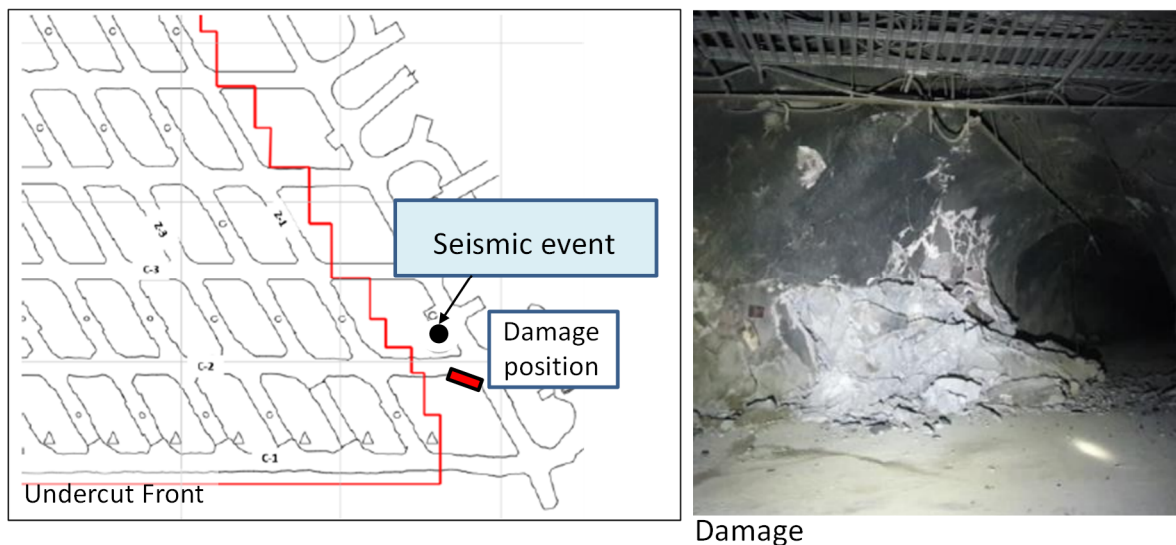


**Figure 13 Damage position**

The ground support installed in the damaged sector includes elements with the characteristics shown in Table 1: 3.0 m long bolts, mesh, and shotcrete. The arrangement of bolts corresponds to those shown in the Figure 1.

After cleaning the sector, a damage thickness of 1.2 m was identified, and a set of geological structural planes parallel to the face where the rock mass slide occurs was observed.

Regarding the bolts, failure due to shear stress was identified and in other bolts on the floor of the previous cut (oxidised failure plane) due to impacts from equipment traffic (refer to Figure 14).

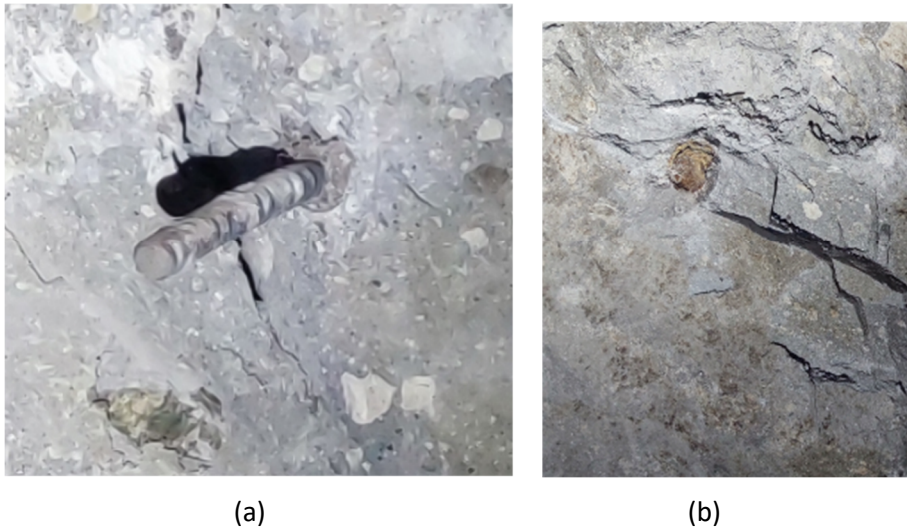


**Figure 14 Bolt failure. (a) Shear bolt failure; (b) Corrosion of bolt in failure**

Figure 15 schematically shows the response of the ground support in the ground, where it can be concluded that the shear stress in the bolts is caused by the sliding of the rock mass through structural planes parallel to the drift.

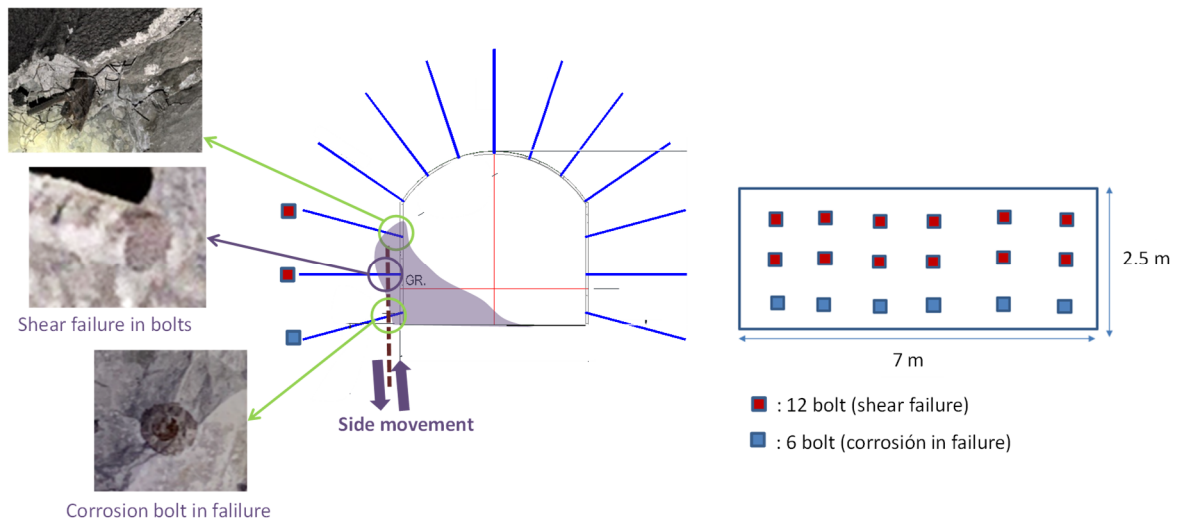


**Figure 15 Support failure mode**

No field information was observed to estimate the ejection velocity, therefore, considering the level of damage, the lowest of the recorded values (2 m/s) in Table 3 will be considered for  $v_e$ .

If the FS is estimated for this case, we obtain:

$$Dynamic\ Load = \frac{1}{2} \times 1.2 \times 2.7 \times 2^2 = 6.5\ kJ/m^2 \tag{10}$$

$$Energy = \frac{22 \times 0.4 \times 12}{7 \times 2.5} = 6.0\ kJ/m^2 \tag{11}$$

$$FS \sim 0.9 \tag{12}$$

From the analysis carried out, the following can be concluded:

- The statistics of combinations of the rockburst events magnitude–energy (Figure 7) shows that for an event of  $M_w 1.4$  and energy of  $2.6 \times 10^5$  J such as that of this rockburst, no damage happens in the bolts, mesh and shotcrete ground support as the one installed by design.
- Therefore, the occurrence of the damage is explained by the sliding of the rock mass through geological structural planes parallel to the drift that creates shear stress in the bolts, limiting the capacity of the support (FS around 0.9), which explains the failure observed in the field.

## 4 Changes to increase the Factor of Safety

Over time, changes have been implemented in the geometry and steel quality of the support elements to improve the response of the ground support, increasing the energy dissipation capacity of the ground support (energy available in the safety factor). These changes have been based on deficiencies observed in the field.

For the system that makes up the bolt with its external anchor plate–nut, the failure of the plate was detected in the field (deformation of the central perforation) which caused the nut to pass through it. The nut also got stuck in the bolt shoulders, affecting the strength of the system (bolt tear out). Examples of this are shown in Figure 16.



**Figure 16 Failures in support system. (a) Plate deformation; (b) Bolt tearing**

To avoid this, the height of the bolt shoulders was increased, the height of the nut was increased, with which a greater grip or bolt–nut contact surface was sought, the thickness was increased and the steel quality of the plate changed. This modification began to be implemented as of 2012 in all the drifts of the mine and as a back-analysis, and this type of failure has not been observed again (Rojas et al. 2020).

In order to increase the energy dissipation capacity of the ground support system, starting in 2015, a 25 mm diameter bolt in A630-420H steel quality began to be included, for which work was done on the development of its external plate–nut anchorage, with which, compared to the 22 mm bolt of steel quality A440-280H, the load capacity doubled (16 t versus 34 t) as did the energy dissipation capacity (22 kJ versus 55 kJ).

In order to enhance the ground support system with the 25 mm diameter bolts of A630-420H quality steel, the use of meshes made of high-strength steel was promoted, from which a significant increase in load and energy dissipation capacity has also been achieved compared to the standard galvanised mesh.

Another relevant issue when evaluating the response of the ground support under dynamic loads is the quality of the support installation when the drifts are developed. This development occurs early in their service life when mining has not yet affected them in terms of stress or loads. In this first stage, it is sought that the support designs are correctly installed in the field in order to guarantee in the future (several years later) that the support elements can fulfill their intended reinforcement and retention roles.

The quality of the support installation positively or negatively impacts the response of the support under dynamic loads. That is why the installation quality of the support system is critical.

Today, at the El Teniente mine, the geomechanics team are dedicated to completing the inspection of the quality of the support installation as part of the technical inspection of works. In this manner, the team seeks to contribute by identifying deviations that could negatively affect the ground support response in the future, promoting good practices in the field and creating spaces to test other types of ground support elements or modifications in designs or construction sequences, depending on the problems identified in the field (Parraguez & Celis 2022).

## 5 Conclusion

As stated, carrying out an analysis of the ground support response is quite complex due to the number of variables involved and the difficulty quantifying them. However, at El Teniente mine, an analysis method has been developed that, with the assumptions described here, has allowed a process to correlate a FS with evidence of field damage.

The challenge remains to advance in the development of instrumentation that allows quantification of the dynamic loads, the load transfer to the ground support system and how it is distributed among the different elements. It is also necessary to define damage halos in the ground support, since the repairs are currently only aimed at areas with visible damage, not including an environment where the ground support has not reached failure but has lost part of its loading and energy dissipation capacity.

The field observations as a back-analysis after the rock bursts has led to the introduction of changes in ground support systems to improve their response to dynamic stresses. In turn, they have promoted the development of new elements to increase the energy dissipation capacity of ground support designs and the formation of a geomechanical specialist team to support the management of the quality of the support installation in the field.

## Acknowledgement

We thank the Mining Resources and Development Management of El Teniente Division for the authorisation and publication of this document.

## References

- Celis, S 2020, *Rockburst Investigation October 2020 Block 1 Esmeralda Sur Mine*, Codelco internal report.
- Constanzo, H, Parraguez, R & Balboa, S, Bustamante, J & Celis, S 2023, *Causal analysis Rockburst February 2023 Pacífico Superior Mine*, Codelco internal report.
- Parraguez, R & Celis, S 2022, *Conceptualization of the Support and Quality Unit of the Operational Geomechanics Superintendent*, Codelco internal report.
- Rojas, E, Muñoz, A & Celis, S 2015, *Energy, Deformation and Corrosion in Support Elements and General Guidelines for Design Support*, Codelco internal report.
- Rojas, E, Parraguez, R, Díaz, J & Celis, S 2020, *Lessons Learned at Pilar Norte Mine*, Codelco internal report.
- Van Sint Jan, M 2005, *Analysis of the Behavior of the Fortification in the Rock Burst of August 30, 2005*, Codelco internal report.

